NASA

Health Monitoring of a Rotating Disk Using a Combined Analytical-Experimental Approach

Ali Abdul-Aziz, Mark R. Woike, John D. Lekki, and George Y. Baaklini
Glenn Research Center, Cleveland, Ohio

NASA STI Program . . . in Profile

Since its founding, NASA has been dedicated to the advancement of aeronautics and space science. The NASA Scientific and Technical Information (STI) program plays a key part in helping NASA maintain this important role.

The NASA STI Program operates under the auspices of the Agency Chief Information Officer. It collects, organizes, provides for archiving, and disseminates NASA's STI. The NASA STI program provides access to the NASA Aeronautics and Space Database and its public interface, the NASA Technical Reports Server, thus providing one of the largest collections of aeronautical and space science STI in the world. Results are published in both non-NASA channels and by NASA in the NASA STI Report Series, which includes the following report types:

*   TECHNICAL PUBLICATION. Reports of completed research or a major significant phase of research that present the results of NASA programs and include extensive data or theoretical analysis. Includes compilations of significant scientific and technical data and information deemed to be of continuing reference value. NASA counterpart of peer-reviewed formal professional papers but has less stringent limitations on manuscript length and extent of graphic presentations.

*   TECHNICAL MEMORANDUM. Scientific and technical findings that are preliminary or of specialized interest, e.g., quick release reports, working papers, and bibliographies that contain minimal annotation. Does not contain extensive analysis.

*   CONTRACTOR REPORT. Scientific and technical findings by NASA-sponsored contractors and grantees.

*   CONFERENCE PUBLICATION. Collected papers from scientific and technical conferences, symposia, seminars, or other meetings sponsored or cosponsored by NASA.

*   SPECIAL PUBLICATION. Scientific, technical, or historical information from NASA programs, projects, and missions, often concerned with subjects having substantial public interest.

*   TECHNICAL TRANSLATION. English-language translations of foreign scientific and technical material pertinent to NASA's mission.

Specialized services also include creating custom thesauri, building customized databases, organizing and publishing research results.

For more information about the NASA STI program, see the following:

*   Access the NASA STI program home page at *http://www.sti.nasa.gov*

*   E-mail your question via the Internet to *help@ sti.nasa.gov*

*   Fax your question to the NASA STI Help Desk at 443–757–5803

*   Telephone the NASA STI Help Desk at 443–757–5802

*   Write to:
    NASA Center for AeroSpace Information (CASI)
    7115 Standard Drive
    Hanover, MD 21076–1320

Health Monitoring of a Rotating Disk Using a Combined Analytical-Experimental Approach

Ali Abdul-Aziz, Mark R. Woike, John D. Lekki, and George Y. Baaklini
Glenn Research Center, Cleveland, Ohio

National Aeronautics and
Space Administration

Glenn Research Center
Cleveland, Ohio 44135

September 2009

Health Monitoring of a Rotating Disk Using a Combined Analytical-Experimental Approach

Ali Abdul-Aziz, Mark R. Woike, John D. Lekki, and George Y. Baaklini
National Aeronautics and Space Administration
Glenn Research Center
Cleveland, Ohio 44135

Summary

Rotating disks undergo rigorous mechanical loading conditions that make them subject to a variety of failure mechanisms leading to structural deformities and cracking. During operation, periodic loading fluctuations and other related factors cause fractures and hidden internal cracks that can only be detected via noninvasive types of health monitoring and/or nondestructive evaluation. These evaluations go further to inspect material discontinuities and other irregularities that have grown to become critical defects that can lead to failure. Hence, the objectives of this work is to conduct a collective analytical and experimental study to present a well-rounded structural assessment of a rotating disk by means of a health monitoring approach and to appraise the capabilities of an in-house rotor spin system.

The analyses utilized the finite element method to analyze the disk with and without an induced crack at different loading levels, such as rotational speeds starting at 3000 up to 10 000 rpm. A parallel experiment was conducted to spin the disk at the desired speeds in an attempt to correlate the experimental findings with the analytical results. The testing involved conducting spin experiments, which covered the rotor in both damaged and undamaged (i.e., notched and unnotched) states. Damaged disks had artificially induced through-thickness flaws represented in the web region ranging from 2.54 to 5.08 cm (1 to 2 in.) in length. This study aims to identify defects that are greater than 1.27 cm (0.5 in.), applying available means of structural health monitoring and nondestructive evaluation, and documenting failure mechanisms experienced by the rotor system under typical turbine engine operating conditions.

Introduction

Health monitoring of rotating components in aircraft engines continues to generate high interest among the engine companies and government institutions to improve safety and to lower maintenance costs. The ideal health monitoring system must comply with certain requirements, and among them are having (1) a sensor system that is capable of sustaining normal function in a harsh environment; (2) the ability to transmit a signal if a detected crack in the component is above a predetermined length, but below a critical length that would lead to failure; and (3) the ability to act neutrally upon the overall performance of the engine system and not interfere with engine maintenance operations. At present, nondestructive evaluation (NDE) techniques are used to perform periodic inspections and may lead to major overhauls to discover any cracks that may have formed to prevent catastrophic failure (burst) of the engine. The lowest cost NDE technique is fluorescent penetrant inspection (FPI). However, FPI often fails to disclose cracks that are tightly closed during rest or that are below the surface. The NDE eddy current system is more effective at detecting both crack types, but requires careful setup and operation, while allowing only a small portion of the disk to be practically inspected. Therefore, the need for more reliable diagnostic tools and high-level techniques for damage detection and health monitoring of rotating components are vital to maintaining engine safety and reliability and for life assessment (Ref. 1).

All of the aforementioned concerns are considered high priorities to the NASA Aviation Safety Program (AvSP), which intends to develop and demonstrate technologies that will contribute to a reduction in the aviation fatal accidents and help improve safety as a whole. This ambitious program is a partnership that includes NASA, the Federal Aviation Administration (FAA), the aviation industry, and the Department

of Defense (Ref. 2). In support of these ventures, the Optical Instrumentation and NDE Branch at the NASA Glenn Research Center at Lewis Field is actively involved in developing capabilities to address the development of specific health monitoring technologies to detect rotor damage prior to any catastrophic events (Ref. 3). The approach taken is to run controlled spin tests that can facilitate the application of various sensing technologies for in situ detection of rotor damage (Refs. 4 to 8). Testing will include performing systematic evaluations of crack detection techniques through the implementation of highly controlled crack initiation and growth tests on subscale spinning rotors up to 46 cm (18 in.) in diameter at 10 000 rpm. Crack detection techniques have been studied by many researchers (Refs. 9 to 11), where the vibration response of a cracked rotor passing through the critical speed is examined utilizing a simple hinge model for small cracks. Bently (Ref. 9) presented a rotor crack detection procedure based on the startup and shutdown vibration monitoring. Additional relevant data concerning the state-of-the-art vibration methodologies related to cracked structures can be found in References 7 and 8.

This report presents an overview of an assessment of a rotor disk spin system health monitoring capability and a discussion of the results obtained from a joint analytical and experimental study. The study included spin testing of a rotor disk 23.495-cm (9.25-in.) in diameter with and without a crack. The disk was operated at various speeds and a detailed NDE-finite element analysis (FEA) examination is conducted. The results are focused on finding the changes in maximum radial deflections and changes in the blade tip displacement as a function of rotational speed and crack characteristics (crack size and location) to make detection feasible.

Analytical-Experimental Approach

Earlier studies to investigate various crack detection techniques considered a flat disk test article to minimize cost and simplify the testing (Ref. 3). The conceptual design utilized a 25.4-cm- (10-in.-) diameter disk with machined teeth to imitate compressor or turbine blades and simulate crack initiation and propagation behavior. The disk consisted of a central region that is counter-bored on both sides to create the rim, web, and bore regions of a typical turbine disk. The machined teeth on the rim simulate blade tip passing, but reduce the effective blade mass-loading on the web and bore of typical blades.

The goal of this design was to induce changes in radial tip displacement in the order of 1.97 µm (0.0005 in.) without disk yielding in an attempt to test the instrumentation, and to then initiate and grow cracks by machining and/or increased rotational speed. Cracks or notches were introduced into the disk geometry at holes near the rim, which resulted in changes in the radial displacements that were very small and experimentally unmeasurable (Ref. 3). Consequently, a new disk shown in Figures 1 and 2 was designed to overcome these concerns and to resemble a turbine disk (Ref. 4), but with a slight increase in manufacturing cost.

Thus, this work re-examines the original flat disk geometry investigated in Reference 3 by updating it to the current disk layout, see Figure 1, and by adding notches through the web thickness and varying the notch location and size. This will help induce detectable changes in displacement and center of mass shift, allowing the study of crack initiation and growth with advanced health monitoring systems by using a reasonably inexpensive test piece and test setups.

The disk shown in Figure 1 has an outside diameter of 23.495 cm (9.25 in.); a bore and an outside rim thickness of 2.54 and 3.175 cm (1 and 1.25 in.), respectively; web thickness of 0.254 cm (0.10 in.); and blade cross section and height are 3.175 by 0.330 cm (1.25 by 0.13 in.) and 0.838 cm (0.33in.), respectively. It has rotor-like blades, totaling 32, evenly spaced around the circumference. Eight holes, of 0.508-cm (0.20-in.) diameter each, were drilled through the disk halfway in the rim. The holes were spaced every 45°, and they were designed for future studies as possible mass attachment points or notch initiation sites. The weight of the disk is 4.88 kg (10.75 lb). Two materials were considered for the manufacturing of the disk: nickel-base superalloy Haynes X–750 (Haynes International, Inc.) and Titanium Grade 2. Test specimens were made for each material, and their physical properties (Ref. 12) are listed in Table I.
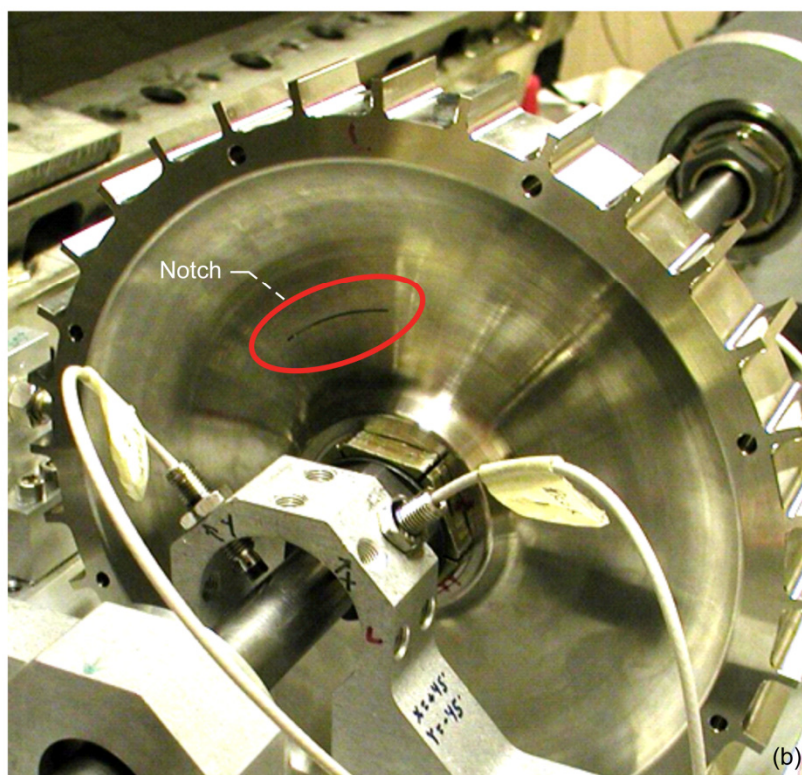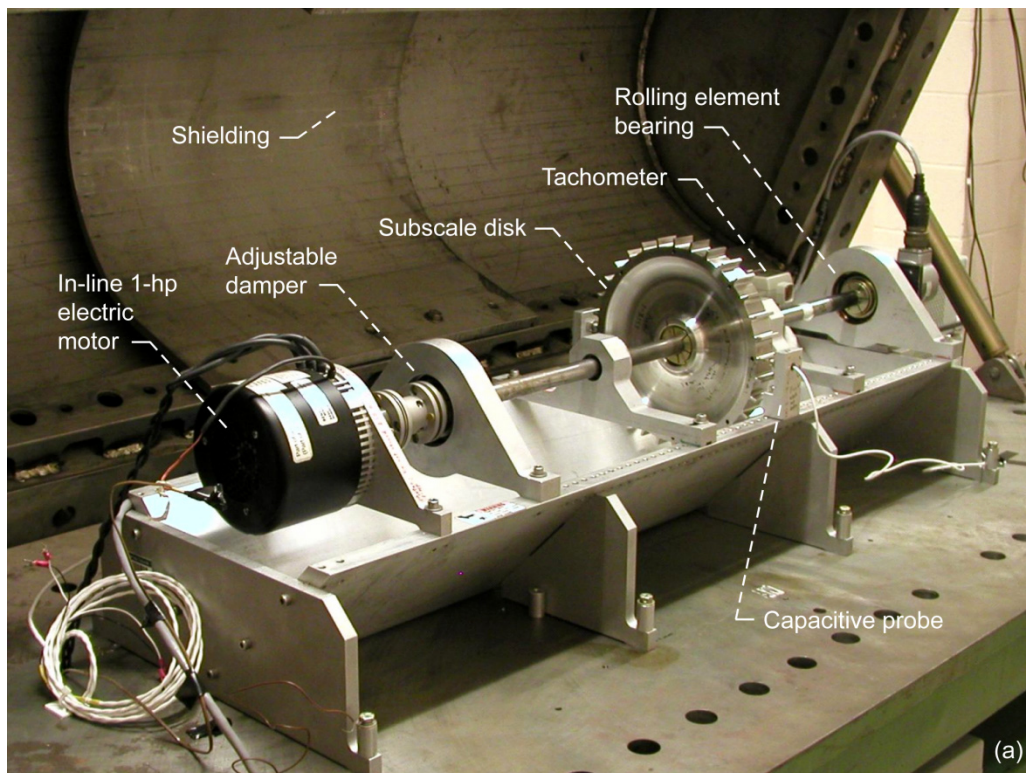
Figure 1.—Rotor spin laboratory. (a) Equipment layout. (b) Test disk specimen with notch.
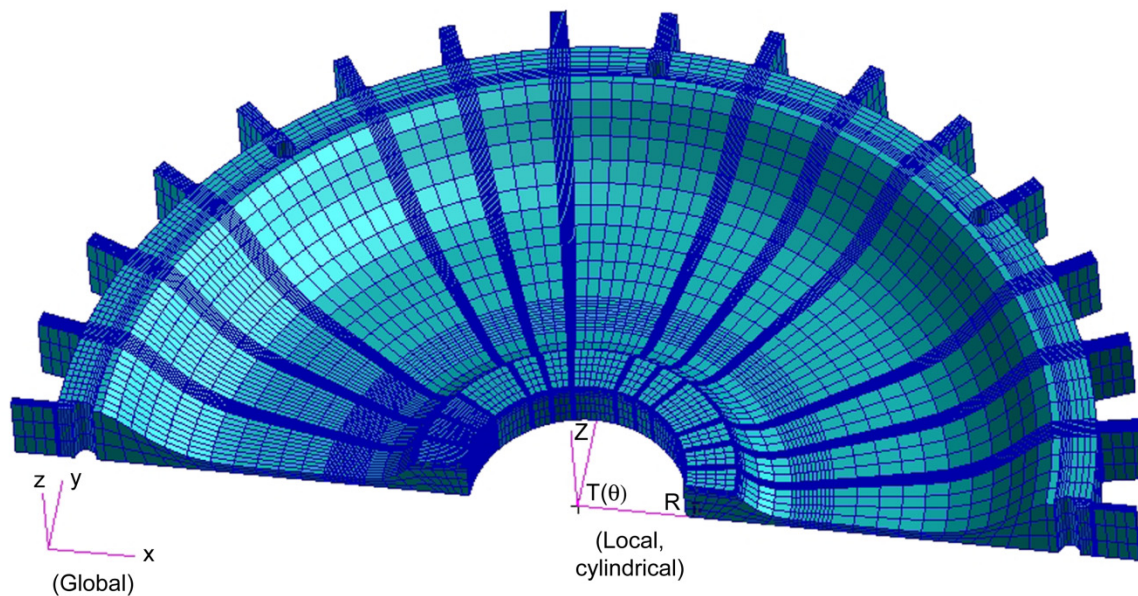
Figure 2.—Rotor FEM.

TABLE I.—PHYSICAL PROPERTIES OF NICKEL-BASE SUPERALLOY
HAYNES X–750 AND TITANIUM GRADE 2

Property	Material	
	Haynes X–750[a]	Titanium Grade 2
Elastic modulus, GPa	214	105
Poisson's ratio	0.31	0.34
Mass density, g/cm^3	8.26	4.50
Tensile strength, MPa	1325	345
Yield strength, MPa	975	276
Thermal expansion coefficient, cm/°C	14.3×10^{-6}	10.1×10^{-6}

[a]Haynes International, Inc.

Finite Element Analysis

The rotating disk has been modeled using MSC/Patran finite element program (Ref. 13). A typical finite element model (FEM) with eight holes and no notches consists of 75 000 nodes and 55 000 eight-node hex elements as shown in Figure 2. The length of the through-thickness notch added in the web was varied from 0.51 to 5.1 cm (0.2 to 2.0 in.). The notch width was usually set to 30.48 μm (0.012 in.). The through-the-thickness notch was cut into the geometry of the FEM, and then meshed. Modeling features such as global and smart size parameters were varied to ensure that numerical stress concentrations did not occur and that similar results were obtained between the solutions of varying mesh sizes.

The model was constrained to replicate the disk attachment to the rotating shaft as represented by the experimental setup (Ref. 6). A local cylindrical coordinate system was created at the center of the disk (see Fig. 2). All of the nodes at the inner radius were constrained in the θ-direction, and the axially centered nodes along the inner radius ring were constrained in the axial Z-direction. Because of symmetry, only 1/8 of the disk was modeled, and all of the nodes at the bottom face were constrained along the global z-axis (see Fig. 2). The calculations were made under linear elastic conditions where the behavior of the material is defined by two material constants, the elastic modulus and Poisson's ratio. The finite element analyses were performed under centrifugal loading conditions experienced by the disk during the spin experiment. The rotational speed during the experiment ranged from a minimum of 3000 to a maximum of 6000 rpm.

Finite element results are illustrated in Figures 3 to 5. Radial stress variation as a function of the rotational speed for the two materials employed in the analysis are shown in Figure 3(a), which also shows the critical segment where material yielding may occur for either disk at an extreme notch size of 5.08 cm. The data shown in Figure 3(a) clearly illustrate the structural limitations of the disk due to the loading applied for both materials. In addition, the figure shows the detailed distribution of stress-displacement profiles to estimate the critical notch size that is suitable for the experimental testing while avoiding the material's yield and premature disk rupture.
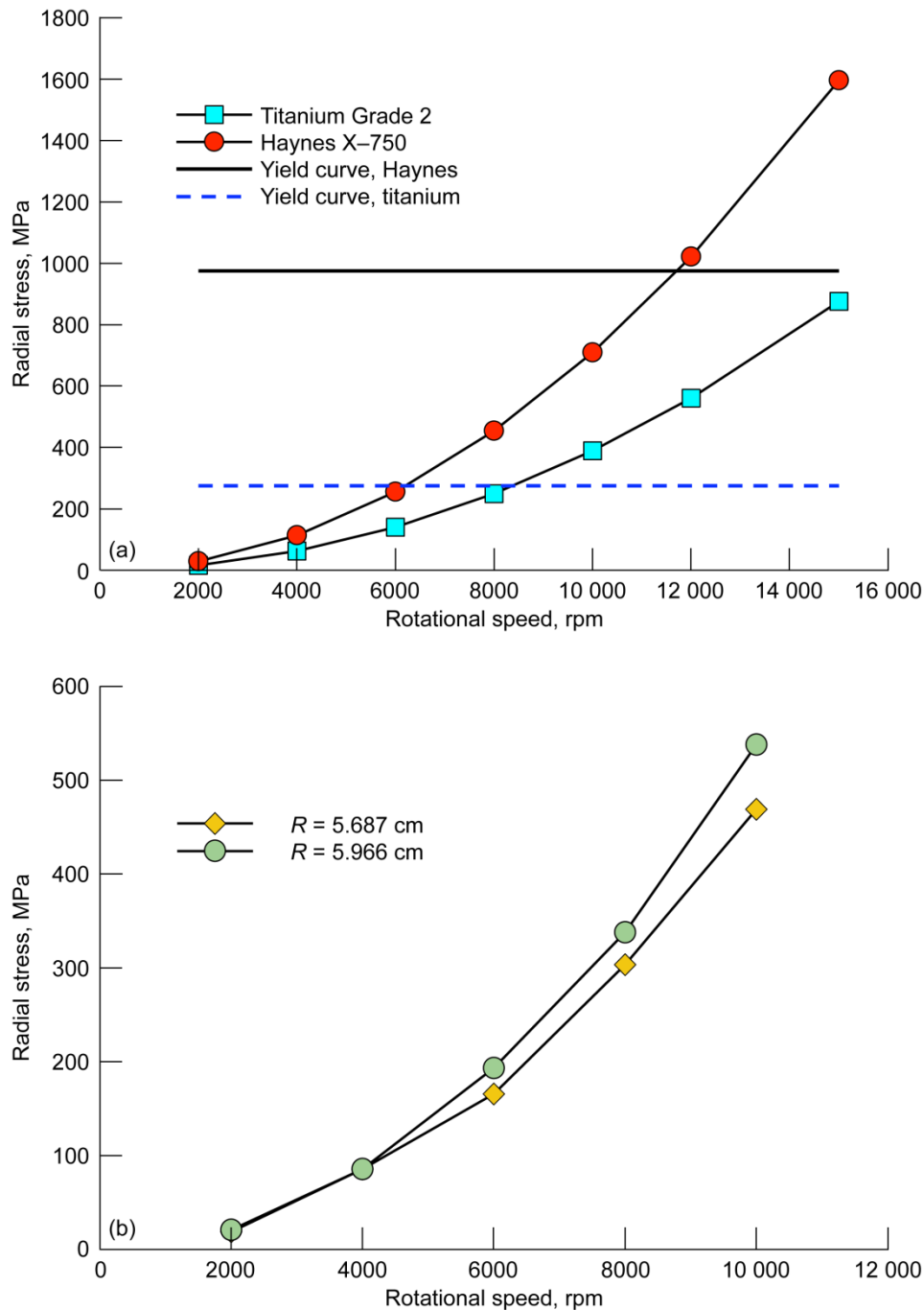

Figure 3.—Radial stress as function of rotational speed. Finite element analysis results. (a) Titanium Grade 2 and Haynes X–750 disks with 5.08-cm-long notch. (b) Haynes X–750 disks with notch at different radii *R* from center of disk.

Figure 3(b) shows the radial stress as a function of the rotational speed for two different locations of the notch. The location of the notch is specified by the radius "*R*" referring to the site of the notch on the web region with respect to the center of the disk. The results showed that the farther the notch site within the web region with respect to the center of the disk and the higher the revolutions per minute are, then the higher is the stress magnitude. High-stress risers are observed at the tip of the notch as projected (see Fig. 4). Furthermore, it is shown that the distribution of the stresses in the disk is very symmetrical, which
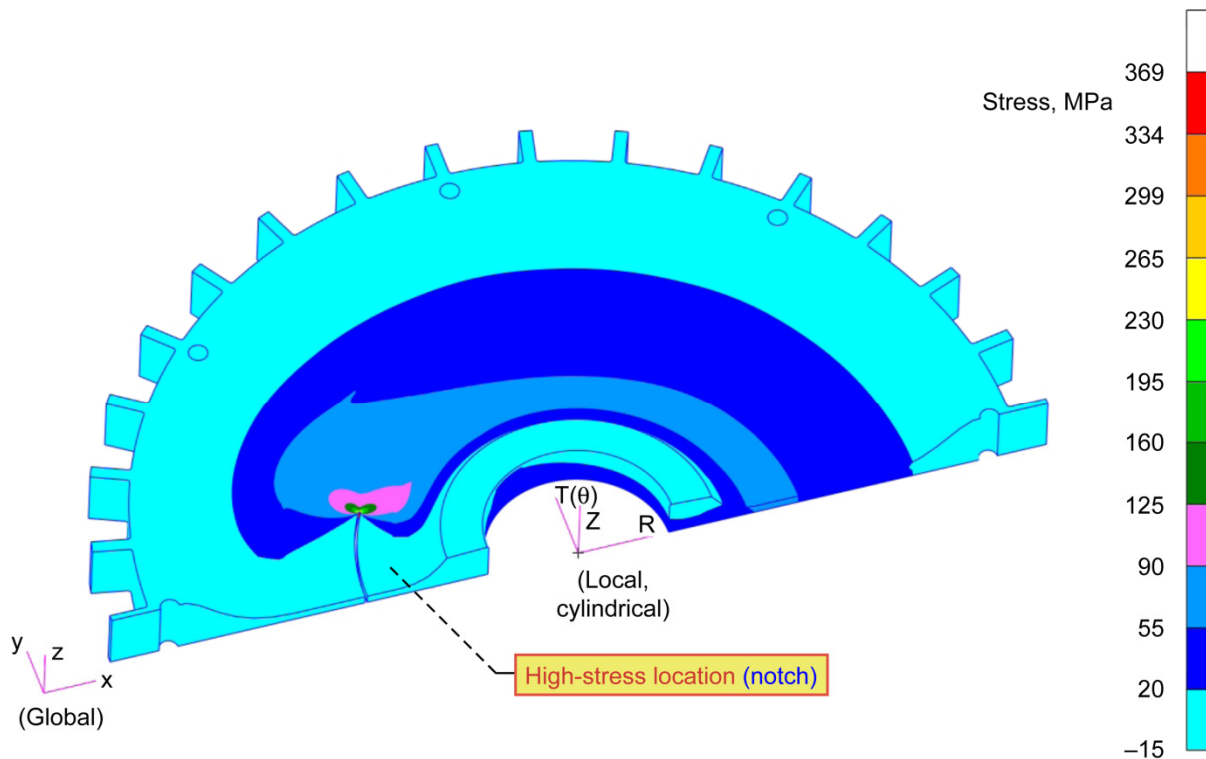

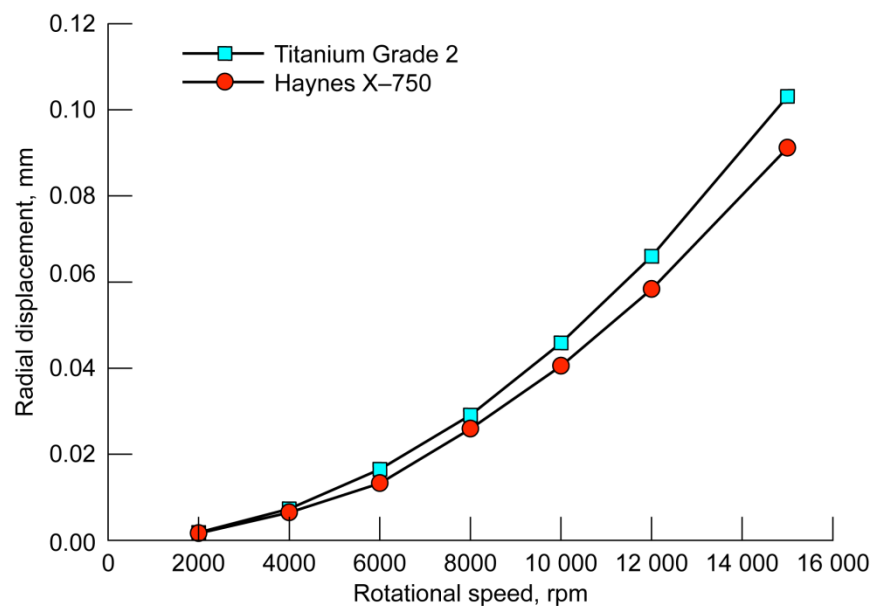Figure 4.—Radial stress distribution at 10 000 rpm (titanium disk).

Figure 5.—Finite element radial displacement as function of rotational speed for Haynes X–750 and Titanium Grade 2 disks with 5.08-cm-long notch.

indicates that the applicability of the boundary conditions to simulate the experimental constraints used in the tests was reasonably accurate. Further, the high-stress state at the notch tip is indicative of a crack initiation site that may eventually grow and lead to a failure of the disk.

Figure 5 represents a comparison of the radial displacement for the disk for both materials, Haynes X–750 and Titanium Grade 2. A lower displacement is reported for the Haynes X–750 compared with that reported for the titanium. This is because of the disparity in the physical properties of each disk material.

NDE–FEA

The NDE–FE-based analysis was carried out to further evaluate the crack site and assess the structural integrity of the disk mainly at the notch position. Among the NDE techniques available to examine the disk unit was the ultrasonic scan; other methods were not practically feasible due to the large size of the object and the complexity of the geometry. The steps to carry out the NDE–FEA process are detailed in the subsequent subsections.

Image Processing and Finite Element (FE) Mesh Generation

The process of constructing an accurate three-dimensional volume from NDE data requires a series of two-dimensional image slices of the specimen under consideration. For a detailed analysis, two-dimensional slices of approximately 0.2-mm spacing are desired, given the accuracy of the NDE system used (ultrasonic imaging) (Ref. 14). While such detail provides an accurate three-dimensional rendering of the whole internal volume, 0.2 mm spacing will create a large database that is very cumbersome for manipulation. Therefore, in this study and for the sake of simplicity, only 10 slices were used, and the separation between each slice was assumed to be 1.25 mm. Additional segmentation was carried out to crop the specimen in order to preserve the data containing the region of interest and minimize the size of the problem, which is the notch area.

Filtering

Because of the noisy nature of the image, some filtering was necessary. The Curvature Anisotropic Diffusion filter, offered by ScanIP/ScanFE (Ref. 14) was used. It is used as a noise reduction filter, rather than a smoothing filter because its purpose is to reduce noise while preserving image features. The Curvature Anisotropic Diffusion filter was applied with a conductance of 5, a time step of 0.0625, and 10 iterations.

Image Segmentation

Segmentation is the process of identifying—within an image—what pixels belong to each object of interest. In this study, several FEMs were considered, differing by mesh density and geometrical definition. The segmentation process itself only influences the geometrical definition of each model. Pixels of values ranging from 121 to 255 were thresholded to create a part representing the test article notch region (Fig. 6).

Mesh Generation NDE–FEA Results

ScanIP/ScanFE was further used to generate a number of finite element meshes based on the three-dimensional segmented image data. The density of meshes generated in ScanFE is closely connected to the image resolution in order to explore convergence of results (field parameters of interest); the image was downsampled (reduced in size) to create two volumes in an attempt to generate, respectively, high- and low-resolution models.
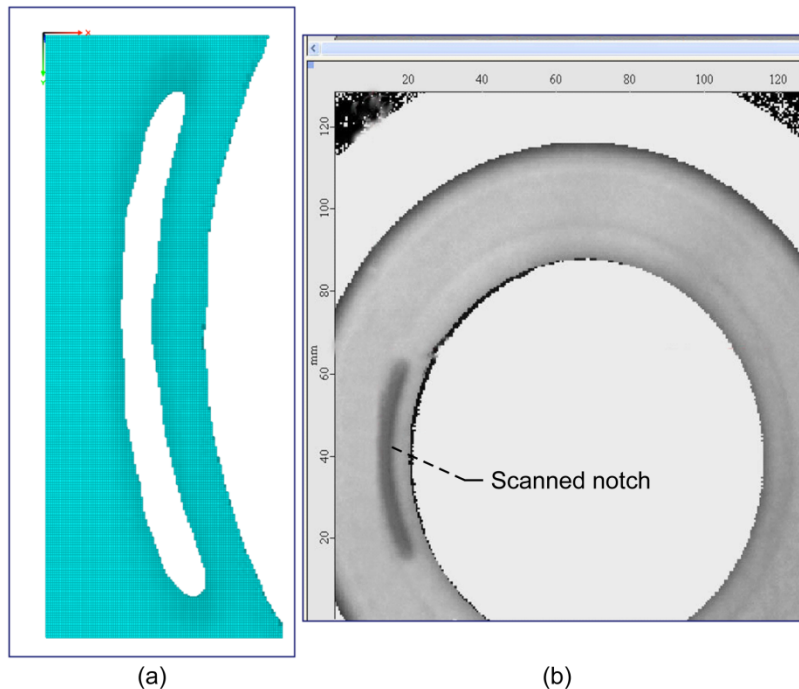
Figure 6.—NDE–FE illustration of notched disk. (a) NDE-generated FEM.
(b) Ultrasonic scan of notched Hayes X–750 disk.

Series of models were generated using 20 iterations of ScanIP's multipart anti-aliasing algorithm, followed by 2 iterations of Laplacian smoothing. The anti-aliasing techniques implemented ensure high accuracy of reconstruction. Mesh optimization parameters ensured that the element quality index reached a value of 0.15, allowing off-surface nodes (within a pixel distance). Figure 6 shows a model that represents a view of the mesh (Fig. 6(a)) along with an image slice of the disk showing the internal features of the notch with the surrounding region and other structural anomalies (Fig. 6(b)). The FEM consists of over 200 000 elements (combination of 8 nodes hexagonal and 4 nodes tetrahedral) and 160 000 nodes. The mesh was carefully modeled to reflect the characteristics of the notch based on the NDE data. Figure 7 is a closeup view of the solid model of the notch showing the corresponding coordinate systems used to constrain the structure.

The three-dimensional CAD model was exported to MSC/Patran (Ref. 13), and an input data file was written for Marc finite element code (Ref. 15) for the analyses. The model was constrained to replicate the disk attachment to the rotating shaft as represented by the experimental setup (Ref. 6). All the nodes at the inner radius were constrained with respect to a local coordinate system (see Fig. 7) in the θ-direction and the bottom and the axially centered nodes along the inner radius ring were constrained along the z-axis. Symmetry constraints were imposed on the other sides along the x- and y-axes to simulate the rest of the disk. Rotational speed was applied to reproduce the spin load.

Results obtained from the analyses are shown in Figure 8. The data represents the stress state in the disk and at the notch region due to the centrifugal force applied. It is shown that the maximum stresses are concentrated as expected at the notch tip indicating that cracks will likely initiate at this site. It should be noted that the stress magnitude shown in Figure 8 does not imply a comparison with the results obtained in Figure 4; it is simply shown for the purpose of confirming the applicability of integrating NDE with FEA and evaluating the disk structural response via another analytical means rather than using FEA data only. Moreover, this also suggests that linking NDE data with FEA can be valuable since they supplement the structural appraisal by supporting the experimental findings. It further should be stated that precision of the results reported is dependent on the accuracy of the NDE technique and the quality of the images collected.
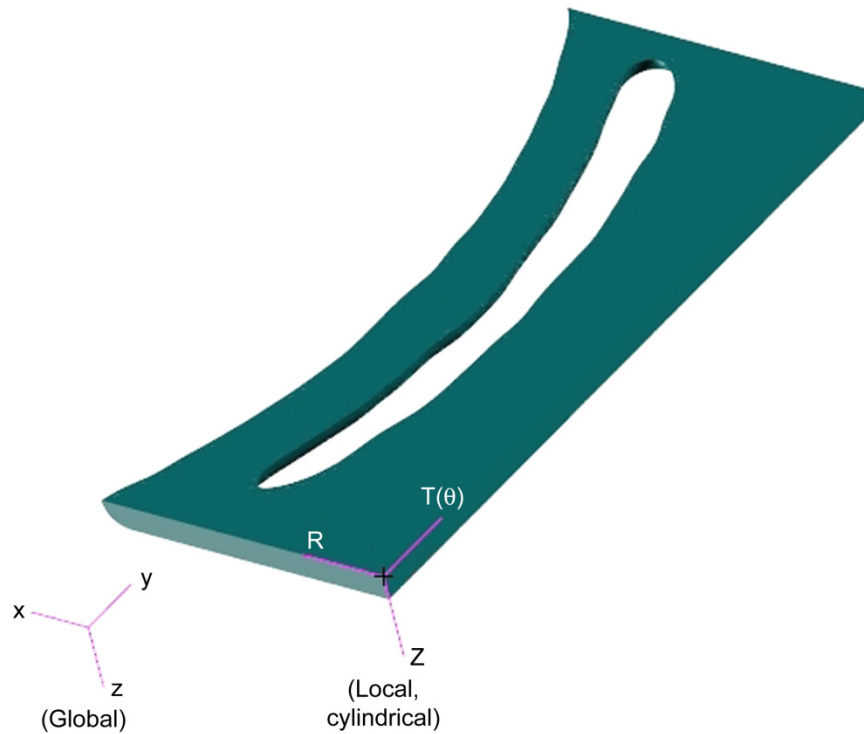
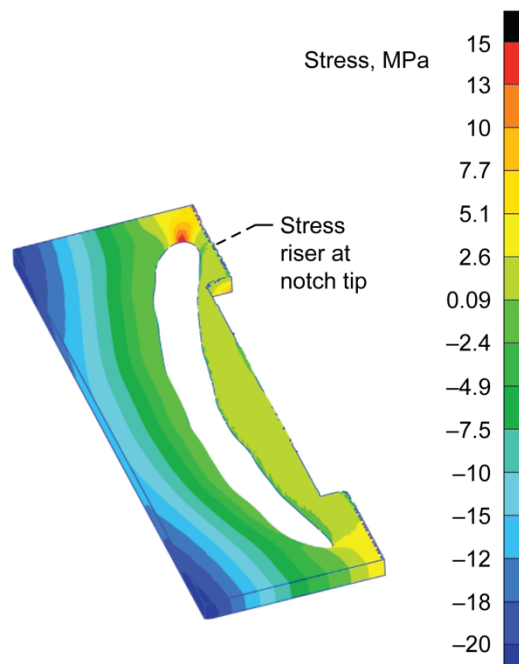Figure 7.—Close up view of notch solid model and designated coordinate systems.

Figure 8.—NDE–FE results of notched Haynes X–750 disk showing radial stress distribution.

Spin Experiment Results and Discussion

To complement the NDE and FEA, experimental testing was carried out in an attempt to identify a crack detection methodology and correlate the findings with theory. It should be noted that experiments were confined to the Haynes X–750 disk (the titanium disk was not tested at this time). A detailed view of the experimental setup used in this study is shown in Figure 1(a). The system has several features. Among those features is an adjustable shaft that allows maneuverability beyond the system's first critical speed. The maximum length was adopted in the experiment because the rotor dynamic calculations indicated a critical speed of 2610 rpm (Ref. 7). The stainless steel shaft length and diameter were 78.105 cm (30.75 in.) and 2.00 cm (0.79 in.), respectively, and the shaft was supported by precision angular contact ball bearings that were assumed to provide isotropic stiffness. The single disk, as seen in Figure 1(b), was mounted at the midspan of the shaft. The disk was designed to safely handle rotational speeds up to 25 000 rpm in the undamaged state (Ref. 7). Also, the capacitive displacement sensors utilized during experimentation were particularly designed, both regarding the hardware and the analysis software, to monitor radial blade tip clearances.

For blade tip clearance measurements, a capacitive sensor system was installed. These types of sensors are based on a direct-current (dc) offset rather than a modulation technique. The dc voltage, in conjunction with the motion of the rotor, allowed the current system to record three channels of data at a rate of 1 MHz per channel. The experimental testing covered running tests under transient and steady-state conditions. This included ramp-up, ramp-down, and cruise conditions. Data such as the blade tip clearance and the corresponding revolutions per minute were collected continuously. The speed applied during these tests ranged from a minimum of 3000 up to a maximum of 6000 rpm with acceleration-deceleration rates of 50 rpm/s. This speed range ensured surpassing the critical speed of 2610 rpm, leading to postcritical state. Experiments covered baseline runs with an undamaged disk and tests with a disk damaged via an artificially induced notch. The notch had a width of 0.381 mm (0.015 in.) due to the wire thickness and burn area of the electric discharge machining (EDM) process. Figure 1(b) shows the disk with the notch; this region was intentionally chosen for the notch location because the FEA results revealed that this section encounters the highest stress level in the disk during the spin operation, see Figure 4. Careful consideration was taken to ensure consistency of the operating condition parameters during the removal-reinstallation process of the disk specimen in both situations, baseline unnotched and notched states.

Upon acquisition, the data were analyzed using specialized in-house software. Figure 9 shows a representative output of the processed experimental data for a typical transient ramp-up–ramp-down 3-min test run at 5000 rpm for the unnotched disk. It also shows the synchronous whirl behaviors in Bode plots, where the amplitude and phase of the system are plotted as functions of rotational frequency. Figure 10 shows comparison of the display image for two runs—notched and unnotched—of the capacitive probe system's postprocessing software. The notch size was confined to 5.08 cm (2 in.) long.

The comparison shows that the Bode plots have changed vastly between the unnotched and notched states. A clear variation is noted: in the notched disk case the curve has peaked at a lower value than the critical speed, whereas in the unnotched disk the curve peaked very closely to critical speed value. Additionally, the trace of vibration vector curves for both cases resembled some similarity except for the difference in higher interference seen in the notched case, which could be attributed to several factors such as defects associated with the presence of the notch.
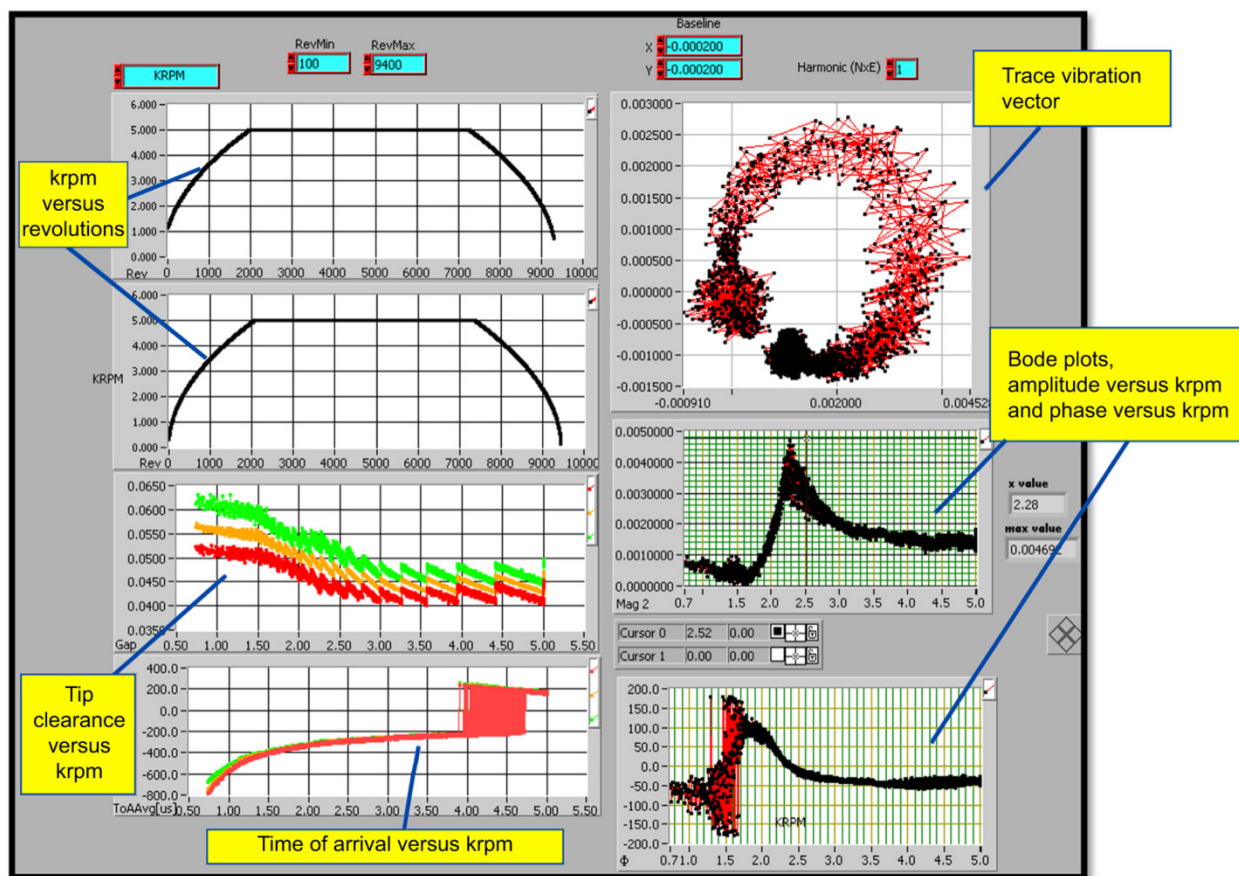
Figure 9.—Typical blade tip clearance data displayed using software associated with capacitive sensors for unnotched disk at 5000 rpm for 3 min.

Further, Figure 10 demonstrates the trace of vibration vectors for both cases; a classical or typical response for the unnotched disk and a relatively nonsmooth, noisy one for the notched disk are noted. This responsive trend might be attributed to either the capacitive probe system or the disk defect due to the notch. This reaction was apparent in the Bode plots and the trace vibration vector plot as well. It can also be related to a possible calibration changes in the overall system caused during the reassembly process of the disk. These calibration and mechanical changes were further indicated by the modifications in the critical speeds and associated maximum amplitudes of whirl as measured by the sensor system.

Additional analyses of the experimental data are presented in Figure 11. Figure 11 is a polar plot showing a comparison of the blade tip clearance response versus rotational speed for three different cases: No notch, Notch1, and Notch2. The references to "Notch1" and "Notch2" are to a small and a large notch, 2.52 and 5.04 cm (1 and 2 in.), respectively. The difference between data from disks with a notch versus those without one is fairly obvious: the changes in the response of the tip clearance in quadrant I suggest that the larger the notch is, the larger is the shift in the polar plot data. The data further show that there is a much higher tip clearance due to the larger notch. In addition, the data could indicate that the loop size is a direct measurement of how much balance is present. The test runs consisted of ramp-up-cruise–ramp-down trends at 3000 rpm and for a 10-min. duration.
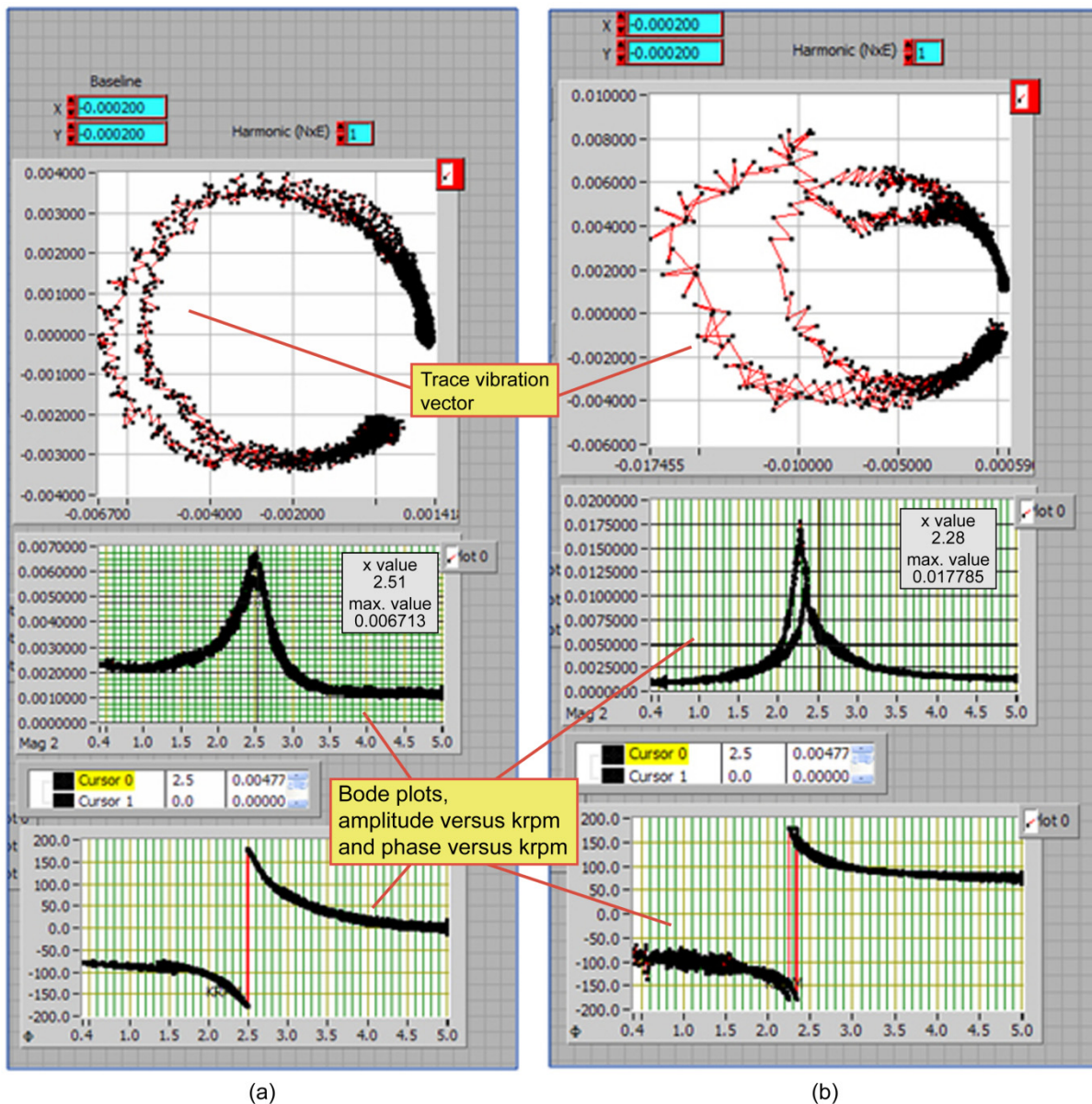
Figure 10.—Comparison of typical blade tip clearance data displayed using software associated with capacitive sensors for disks at 5000 rpm for 3 min. (a) Unnotched disk. (b) Notched disk.
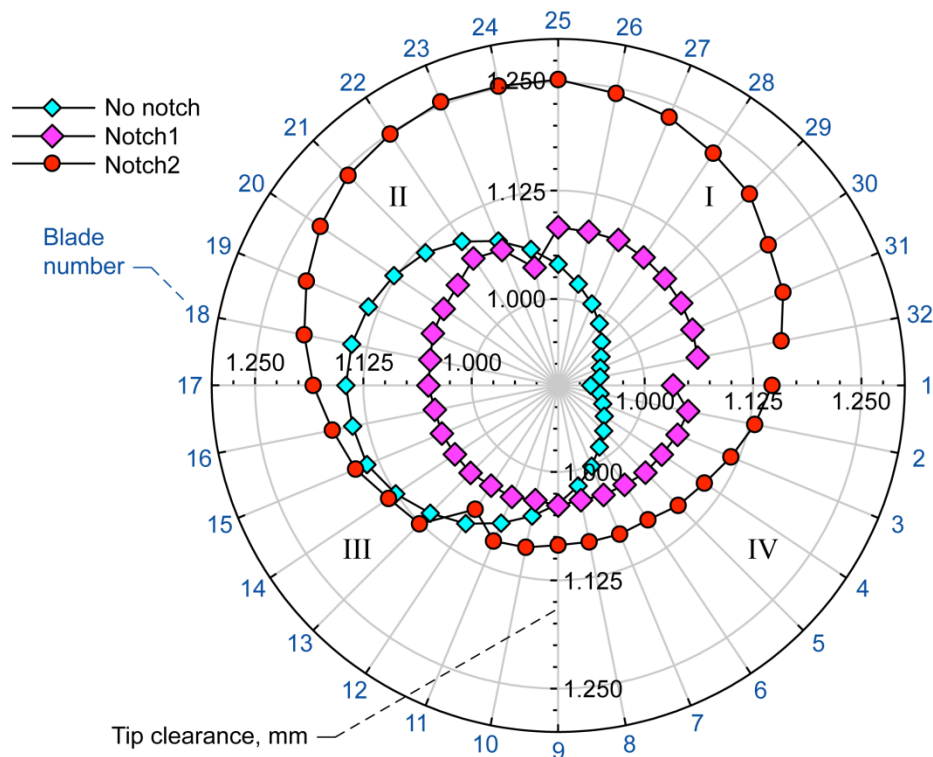
Figure 11.—Polar plot (quadrants I through IV indicated) showing comparison of tip clearance of each blade (32 blades) for unnotched and notched Haynes X–750 disks at 3000 rpm for 10 min.

Conclusions

A health monitoring study of a turbine-engine-like rotor disk was conducted via a combined analytical, experimental, and nondestructive evaluation (NDE) approach. The study involved conducting thorough finite element analyses of the rotor disk to allow physics-based understanding of the localized stress response due to loading conditions and to obtain a clear assessment of the failure mechanism. The analyses included performing calculations of the disk with and without an induced crack or notch at different speed levels, such as 3000 up to10 000 rpm. A parallel experiment to spin the disk at selected speeds (3000 to 5000 rpm) was carried out in attempt to correlate the experimental findings with the analytical results. Supplementary health monitoring verification was performed via integrating NDE statistics with finite element analyses to model the disk flaws using an ultrasonic scan data.

The effects of notch size and location on radial displacement were investigated via finite element analysis (FEA) for various rotational speeds for both materials considered, Titanium Grade 2 and Haynes X–750 nickel-base superalloy. Plots of data showing limitations on the material's yield conditions due to speed and notch size were generated. The NDE information along with FEA offered an additional means of health monitoring by permitting the modeling of the disk flaws. Subsequently, the results obtained confirmed that high stress risers are at the notch tip as anticipated. Experimental data acquired gave ample information about the crack detection scheme applied. It showed that the blade tip clearance tends to be larger upon the existence of a notch, and the polar plots offered more support in showing that the larger the flaw, then the larger is the change in the tip clearance data in the direction of the first quadrant. This may indicate the presence of a defect in the rotating component. Bode plots offered more asserting results concerning the crack detection. They showed that initial spikes in amplitude and phase change do take place prior to reaching the blade critical speed in the presence of a defect.

This study along with prior ones offers a baseline assessment of the effects of the key design parameters on the overall performance of the disk. However, additional work is warranted to reach more conclusive statements regarding the relative gains and benefits to be achieved with respect to durability and applicability of the health monitoring system. Lastly, this work demonstrates that the spin system at NASA Glenn Research Center has the capabilities to provide the necessary means for conducting experiments that would assist in the development of flaw detection and health monitoring schemes for turbine engine components (e.g., rotor disks).

References

1. Abdul-Aziz, Ali: Nondestructive Testing of Ceramic Materials. Mater. Eval., vol. 64, no. 1, 2006, pp. 20–22.
2. Simon, Donald L.: An Overview of the NASA Aviation Safety Program Propulsion Health Monitoring Element. NASA/TM—2000-210348 (AIAA–2000–3624), 2000.
3. Abdul-Aziz, Ali; Trudell, Jeffrey J.; and Baakilini, George Y.: Finite Element Design Study of a Bladed, Flat Rotating Disk to Simulate Cracking in a Typical Turbine Disk: Part II. Proc. SPIE Int. Soc. Opt. Eng., vol. 6176, 2006.
4. Abdul-Aziz, Ali; Trudell, Jeffrey J.; and Baakilini, George Y.: Finite Element Design Study of a Bladed, Flat Rotating Disk to Simulate Cracking in a Typical Turbine Disk. Proc. SPIE Int. Soc. Opt. Eng., vol. 5767, 2005, pp. 298–307.
5. Gyekenyesi, Andrew L.; Sawicki, Jerzy T.; and Baaklini, George Y.: Vibration Based Crack Detection in a Rotating Disk. Part 1—An Analytical Study. NASA/TM—2003-212624/PART1, 2003.
6. Gyekenyesi, Andrew L., et al.: Vibration Based Crack Detection in a Rotating Disk. Part 2—Experimental Results. NASA/TM—2005-212624/PART2, 2005.
7. Drumm, M.J.: Nondestructive, Real-Time Measurement of Cracks in Jet Engine Rotors. 1998. www.testdevices.com Accessed August 13, 2009.
8. Sonnichsen, E.: Real-Time Detection of Developing Cracks in Jet Engine Rotors. IEEE, 0–7803–5846–5/00, 2000. www.testdevices.com Accessed August 13, 2009.
9. Bently, Don: Detecting Cracked Shafts at Earlier Levels. Orbit, July 1982.
10. Sekhar, A.S.; and Prabhu, B.S.: Condition Monitoring of Cracked Rotors Through Transient Response. Mech. Mach. T., vol. 33, no. 8, 1998, pp. 1167–1175.
11. Wauer, Jorg: On the Dynamics of Cracked Rotors: A Literature Survey. Appl. Mech. Rev., vol. 43, no. 1, 1990, pp. 13–17.
12. Holt, John M. (Tim); Mindlin, Harold; and Ho, C.Y.: Structural Alloys Handbook. 1996 ed., CINDAS/Purdue University, West Lafayette, IN, 1996.
13. MSC/PATRAN Graphics and Finite Element Package. Vols. I and II, The MacNeal-Schwendler Corporation, Costa Mesa, CA, 1997.
14. ScanIP/ScanFE. Simpleware Ltd., Innovation Centre, Exeter, UK, 2000–2009.
15. Marc 2007 r1. The MacNeal-Schwendler Corporation, Costa Mesa, CA, 2007.

1. REPORT DATE (DD-MM-YYYY) 01-09-2009	2. REPORT TYPE Technical Memorandum		3. DATES COVERED (From - To)	
4. TITLE AND SUBTITLE Health Monitoring of a Rotating Disk Using a Combined Analytical-Experimental Approach			**5a. CONTRACT NUMBER**	
			5b. GRANT NUMBER	
			5c. PROGRAM ELEMENT NUMBER	
6. AUTHOR(S) Abdul-Aziz, Ali; Woike, Mark, R.; Lekki, John, D.; Baaklini, George, Y.			**5d. PROJECT NUMBER**	
			5e. TASK NUMBER	
			5f. WORK UNIT NUMBER WBS 645846.02.07.03.11.03	
7. PERFORMING ORGANIZATION NAME(S) AND ADDRESS(ES) National Aeronautics and Space Administration John H. Glenn Research Center at Lewis Field Cleveland, Ohio 44135-3191			**8. PERFORMING ORGANIZATION REPORT NUMBER** E-17038	
9. SPONSORING/MONITORING AGENCY NAME(S) AND ADDRESS(ES) National Aeronautics and Space Administration Washington, DC 20546-0001			**10. SPONSORING/MONITOR'S ACRONYM(S)** NASA	
			11. SPONSORING/MONITORING REPORT NUMBER NASA/TM-2009-215675	
12. DISTRIBUTION/AVAILABILITY STATEMENT Unclassified-Unlimited Subject Categories: 01 and 05 Available electronically at http://gltrs.grc.nasa.gov This publication is available from the NASA Center for AeroSpace Information, 443-757-5802				
13. SUPPLEMENTARY NOTES				

14. ABSTRACT

Rotating disks undergo rigorous mechanical loading conditions that make them subject to a variety of failure mechanisms leading to structural deformities and cracking. During operation, periodic loading fluctuations and other related factors cause fractures and hidden internal cracks that can only be detected via noninvasive types of health monitoring and/or nondestructive evaluation. These evaluations go further to inspect material discontinuities and other irregularities that have grown to become critical defects that can lead to failure. Hence, the objectives of this work are to conduct a collective analytical and experimental study to present a well-rounded structural assessment of a rotating disk by means of a health monitoring approach and to appraise the capabilities of an in-house rotor spin system. The analyses utilized the finite element method to analyze the disk with and without an induced crack at different loading levels, such as rotational speeds starting at 3000 up to 10 000 rpm. A parallel experiment was conducted to spin the disk at the desired speeds in an attempt to correlate the experimental findings with the analytical results. The testing involved conducting spin experiments which, covered the rotor in both damaged and undamaged (i.e., notched and unnotched) states. Damaged disks had artificially induced through-thickness flaws represented in the web region ranging from 2.54 to 5.08 cm (1 to 2 in.) in length. This study aims to identify defects that are greater than 1.27 cm (0.5 in.), applying available means of structural health monitoring and nondestructive evaluation, and documenting failure mechanisms experienced by the rotor system under typical turbine engine operating conditions.

15. SUBJECT TERMS
Rotor dynamics; Spin testing; Nondestructive evaluation; Finite element

16. SECURITY CLASSIFICATION OF:			**17. LIMITATION OF ABSTRACT**	**18. NUMBER OF PAGES**	**19a. NAME OF RESPONSIBLE PERSON** STI Help Desk (email:help@sti.nasa.gov)
a. REPORT U	**b. ABSTRACT** U	**c. THIS PAGE** U	UU	20	**19b. TELEPHONE NUMBER** (include area code) 443-757-5802